Journal of Nuclear Materials 404 (2010) 109–115

Contents lists available at ScienceDirect

Journal of Nuclear Materials

journal homepage: www.elsevier.com/locate/jnucmat

First-principles study on dissolution and diffusion properties of hydrogen in molybdenum

Chen Duan [a], Yue-Lin Liu [a], Hong-Bo Zhou [a], Ying Zhang [a], Shuo Jin [a], Guang-Hong Lu [a,*], G.-N. Luo [b]

[a] Department of Physics, Beijing University of Aeronautics and Astronautics, Beijing 100191, China
[b] Institute of Plasma Physics, China Academy of Sciences, Hefei 230031, China

ARTICLE INFO

Article history:
Received 20 November 2009
Accepted 16 June 2010

ABSTRACT

Employing a first-principles method, we have investigated dissolution and diffusion properties of hydrogen (H) in molybdenum (Mo), one of potential candidates for plasma facing materials in a nuclear fusion Tokamak. We show that single H atom is energetically favorable sitting at the tetrahedral interstitial site (TIS) instead of octahedral interstitial site and diagonal interstitial site. This can be confirmed by the electron localization function result. Bader charge analysis suggests that the bonding between H and surrounding Mo is mainly ionic mixed with slight covalent component. Double H atoms tend to be paired up at the two neighboring TIS's along the ⟨1 1 0⟩ direction with the distance of ~0.221 nm and the binding energy of 0.03 eV. This suggests a weak attractive interaction between H atoms, with the implication that self-trapping of H and thus formation of the H_2 molecules are quite difficult in an intrinsic Mo environment. We demonstrate that the diffusion barrier of H that jumps between the TIS's is 0.16 eV, and the dissolved concentration of H in the intrinsic Mo is 2.6×10^{-8} at a typical temperature of 600 K. The diffusion coefficients of H, D, and T are different due to the different masses, which are calculated to be 1.3×10^{-7} m^2/s, 9.2×10^{-8} m^2/s, and 7.5×10^{-8} m^2/s at 600 K.

1. Introduction

The interaction of hydrogen (H) with metals is of great scientific and technological interest, having a broad range of applications including H-storage applications [1,2], H embrittlement in metals [3], and H-wall materials interaction in a nuclear fusion reactor [4–6]. At present, metal is being used as an important candidate of plasma facing material (PFM) in the fusion reactor, which generates one of the important alternative clean energy resources in the future [7]. The PFM is exposed to extremely high fluxes of H isotope (deuterium–tritium) ions [4,8,9], which can give rise to H accumulation, bubble formation, and blistering. This is a common cause for degrading mechanical properties of the PFM [4]. Thus, the PFM must withstand "H" and other radiation damage to keep its intrinsic mechanical properties and structural strength. On the other hand, the retention control of H isotopes deuterium (D) and tritium (T) is a major subject for the PFM in the fusion reactor. The lower retention of D and T in the PFM is greatly expected. Consequently, understanding the interaction between H and a metal PFM has a direct impact on design and preparation of the PFM in the fusion reactor.

Recently, both theoretical and experimental studies [5,6,8,9] focused on the interaction between H and tungsten (W), which is considered as one of the most promising PFMs in the fusion Tokamak such as ITER. The H behavior in Molybdenum (Mo), however, generally received less attention in comparison with W. Mo and Mo-alloys are also regarded as one of the promising PFM candidates because of their low sputtering erosion and good thermal and mechanical properties [10–12]. Both W and Mo are high-Z refractory metals with similar physical properties. The atomic number of Mo is 42 and its valence electron structure is $4d^5 5s^2$. The melting point of Mo is 2610 °C, 800 °C lower than that of W. However, Mo has several characteristic properties in comparison with W. As compared with W: (i) lower melting point of Mo makes it easier to be forged; (ii) Mo has lower physical sputtering rate and lower sputtering threshold; (iii) The erosion rate of Mo is much lower, giving rise to longer life as the PFM [13]; and (iv) H has higher diffusivity and lower solubility in Mo, leading to lower H retention [14–16]. These characteristics make Mo as an important substitutional candidate material for the W-based PFM.

H blistering in Mo is considered as one of important issues in designing Mo as a PFM. Experimental studies have shown that the bombardment of high flux of H isotope ions (D) on single crystal [14] as well as polycrystalline Mo [10] will cause H accumulation and blistering in Mo. H retention in Mo is another important issue that must be taken into account, which is closely associated with H blistering. Tanabe et al. have examined the retention behavior of D implanted in Mo [17]. They found that D behavior in Mo is obviously different below and above 500 K. Nagata and Takahiro

* Corresponding author. Tel./fax: +86 10 82339917.
E-mail addresses: jinshuo@buaa.edu.cn (S. Jin), lgh@buaa.edu.cn (G.-H. Lu).

0022-3115/$ - see front matter © 2010 Elsevier B.V. All rights reserved.
doi:10.1016/j.jnucmat.2010.06.029

have investigated trapping of D in W and Mo using ion beam analysis techniques [14]. It is shown that there exists an obvious difference about the D retention content between W and Mo at a temperature range. Recently, Hoshihira et al. studied systematically the T retention in Mo and found blistering phenomenon occurs obviously [18,19]. Further, the diffusion coefficients for H, D and, T in Mo as well as other metals are different due to the mass difference [20], leading to different diffusivities and retention.

Defects are shown to play an essential role in the H trapping in Mo and W as well as other metals. In the earlier studies, the effective medium theory (EMT) has been used to calculate the solution and the vacancy trapping properties of the H isotope ions in Mo [21] and other transition metals [22–27]. Meanwhile, comparison of the theoretical calculations with the experimental measurements shows that H isotope ions have been found to strongly interact with defects in Mo. For example, the vacancy is shown to easily trap H atoms and the trapping energy is still favorable up to six H atoms [22]. A microscopic vacancy trapping mechanism of H in W has been proposed in terms of "an optimal electron density" [28]. On the other hand, H has been also shown to assist vacancy formation in metals such as Mo, W, Ni, Cr, Pd and Al [29–32], which will in turn further enhance the H trapping. The relevant results have been reviewed systematically by Condon and Schober[4] and Fukai [33].

In order to further understand the H interaction with Mo, in this paper, we investigate the structure, energetics and diffusion of H in Mo using the first-principles method. The dissolved concentration and the diffusion coefficient of H according to the empirical theory are calculated based on the first-principles calculations. These results can be served as a first step to further study the H interactions with defects in Mo so as to understand H blistering mechanism in a microscopic atomic level.

2. Computational methods

Our first-principles calculations were performed using the pseudopotential plane wave method implemented in the VASP code [34,35] based on the density functional theory (DFT). We used the generalized gradient approximation of Perdew and Wang [36] and projector augmented wave potentials [37] with a plane wave energy cutoff of 350 eV. During geometry optimization, a bcc-Mo supercell of 128 atoms is used with the side length of 1.264 nm, and the Brillouin zone are sampled with $3 \times 3 \times 3$ k-points grid according to the Monkhorst–Pack scheme [38]. The calculated equilibrium lattice constant is 0.316 nm for bcc Mo, in good agreement with the corresponding experimental value of 0.315 nm [39]. Both supercell size and atomic positions were relaxed to equilibrium, and energy minimization was converged until the forces on all the atoms are less than 10^{-2} eV/nm.

The solution energy of the interstitial H atom in the intrinsic Mo is defined as

$$E_{\mathrm{H}}^{s} = E_{N\mathrm{Mo,H}} - NE_{\mathrm{Mo}} - \frac{1}{2}E_{\mathrm{H}_2}, \tag{1}$$

where $E_{N\mathrm{Mo,H}}$ is the energy of the supercell with N Mo atoms and one H atom, E_{Mo} is the energy of an ideal bulk Mo atom, and $\frac{1}{2}E_{\mathrm{H}_2}$ is one-half of the energy of a H_2 molecule, which is -3.36 eV according to the present calculation.

The binding energy E_b of two H atoms in the intrinsic Mo is defined as

$$E_{2\mathrm{H}}^{b} = 2E_{1\mathrm{H}} - E_{2\mathrm{H}} - E_{ref}, \tag{2}$$

where $E_{1\mathrm{H}}$ and $E_{2\mathrm{H}}$ are the energies of the supercell with one tetrahedral interstitial site H atom only and two H atoms, respectively, and E_{ref} is the energy of the corresponding supercell without H atoms. Here, negative value of binding energy indicates repulsion between H atoms, while positive one indicates attraction.

3. Results and discussion

3.1. Dissolution of H in Mo

We first examine the stability of single H atom in the intrinsic Mo. For single H atom, in addition to considering two high symmetry cases of the tetrahedral interstitial site (TIS) and octahedral interstitial site (OIS), we also select the diagonal interstitial site (DIS), which sits between two neighboring TIS's. Fig. 1 shows the atomic structure and valence electron density distribution of H at the TIS, the OIS, and the DIS, respectively. A single H is shown to be energetically favorable occupying the TIS with a solution energy of 0.62 eV in reference to one-half of the energy of a H_2 molecule (-3.36 eV), with the positive value indicating that the dissolution of H in Mo is endothermic. This is consistent with the existing experimental results of 0.54 eV [40] and 0.56 eV [41]. The slight overestimation should be mainly due to failing to consider effect of the vacancy-related defects, which can effectively trap H atom and thus facilitate its dissolution [6,31]. H in the OIS and the DIS exhibit the solution energies of 0.94 eV and 0.74 eV, respectively, less stable than the TIS.

Similar to our previous studies [28,42], the H solution behavior in a metal can be physically understood in terms of "an optimal electron density" [28]. Generally, the H solution energy will monotonically decrease with decreasing electron density until reaching an optimal electron density [28,43,44]. Since the electron density everywhere in the intrinsic Mo, as well as in most metals, is much higher than this value, we should find the lower electron density sites with lower solution energy. In the intrinsic Mo, the present results show that the TIS has an electron density of $\sim$250 electron/nm^3 which is between those of $\sim$230 electron/nm^3 and $\sim$260 electron/nm^3 of the OIS and DIS. The H solution energy, however, is found to be lower at the TIS than the OIS and the DIS. Hence, in addition of the electron density effect, an additional atomic structure effect also plays a role, making the solution energy of the TIS lowest in the three interstitial cases.

We further examine the charge transfer between three kinds of interstitial H atoms and Mo, according to Bader charge analysis based on Atom in Molecule (AIM) theory [45] with a grid-based algorithm [46,47]. In this analysis, based on the charge density distribution, the real-space is partitioned into several subspaces associated with each atom. The boundary of an atom is delimited by the zero-flux surface of the charge density gradient vector field on which the charge density reaches minimum perpendicular to the surface. The integrated charge enclosed within the zero-flux surfaces can be taken as a good approximation of the charge of an atom.

Table 1 and Fig. 2 present the Bader charge of the H atom and six neighboring Mo atoms for all the three interstitial cases. In all these cases, the interstitial H atom obtains the electron from the host Mo atom and becomes negatively charged, with the Bader charge of approximately -0.8e, qualitatively in accordance with the previous EMT study that H in metal can be regarded as a screened H^- [48]. For the TIS case, the Bader charge of H is calculated as -0.79e. All the Bader charge are +0.12e for the 1NN Mo atom (Nos. 1, 2, 5, and 6), with a shorter distance 0.185 nm from H, while the Bader charge becomes almost zero for the 2NN Mo (Nos. 3 and 4). For the OIS case, the Bader charge of H, 1NN Mo atoms (Nos. 5 and 6), and 2NN Mo atoms (Nos. 1, 2, 3, and 4) are -0.77e, +0.11e, and +0.09e, respectively. This indicates that H interacts with both 1NN and 2NN atoms but with a relatively stronger interaction with 1NN atoms. As for the DIS case, H (with

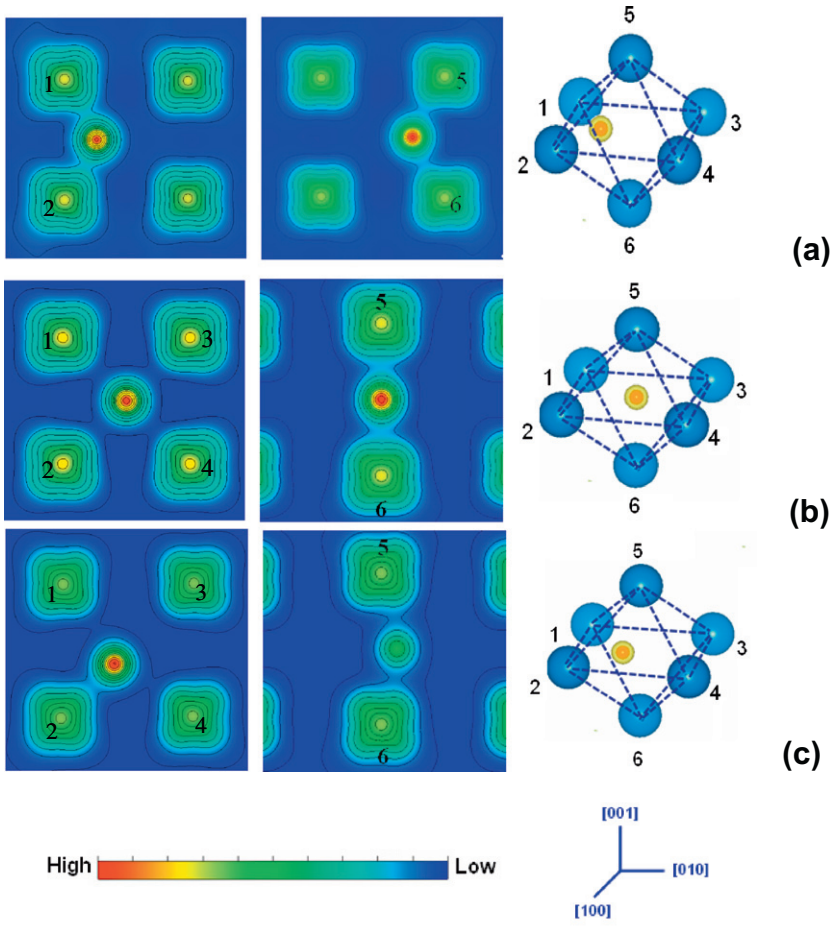

Fig. 1. Valence electron density distribution maps along the (0 0 1) and the (1 0 0) planes, and the corresponding atomic configurations for (a) the TIS, (b) the OIS, and (c) the DIS, respectively.

Table 1
Calculated Bader charge (in the unit of e) for H atom and six neighboring Mo atoms and the corresponding distances between H and Mo d_{H-Mo} in the unit of nm.

Site	TIS		OIS		DIS	
	d_{H-Mo} (nm)	Bader charge (e)	d_{H-Mo} (nm)	Bader charge (e)	d_{H-Mo} (nm)	Bader charge (e)
H		−0.79		−0.77		−0.77
Mo(1)	0.185	+0.12	0.223	+0.09	0.228	+0.10
Mo(2)	0.185	+0.12	0.223	+0.09	0.184	+0.15
Mo(3)	0.284	−0.02	0.223	+0.09	0.271	+0.02
Mo(4)	0.284	−0.02	0.223	+0.09	0.228	+0.10
Mo(5)	0.185	+0.12	0.175	+0.11	0.178	+0.10
Mo(6)	0.185	+0.12	0.175	+0.11	0.178	+0.10

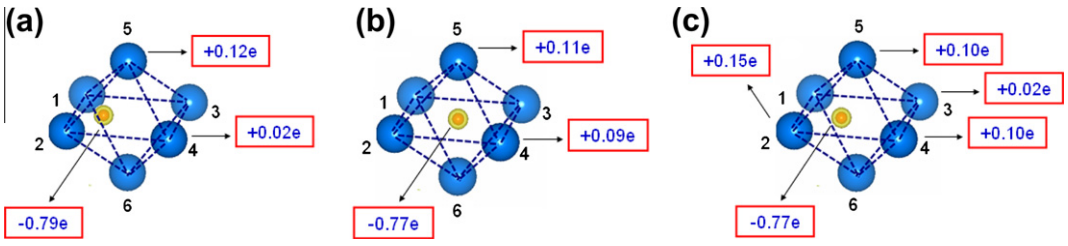

Fig. 2. The Bader charge for H in (a) TIS, (b) OIS, and (c) DIS, respectively.

the Bader charge +0.77e) mainly interacts with five neighboring Mo atoms (Nos. 1, 2, 4, 5, and 6). The Bader charge of Mo (2) is the largest (+0.15e), and other four neighboring Mo atoms (Nos. 1, 4, 5, and 6) are almost the same (+0.10e). For the Mo atoms with a farther distance from H (e.g. atom 3, 0.272 nm), the Bader charge approximates to zero. The Bader charge results suggest that H

interacts mainly with the neighboring Mo with an ionic-covalent mixing bond but containing only slight covalent components.

The electron localization function (ELF) is a useful tool that can distinctly reflect the chemical bonding character in metals and metal-alloys [49,50]. The value of ELF can provide the probability distribution of paired electrons and better distinguish different bonding situations for electrons in comparison with plain valence electron density distribution. In the previous studies, different kinds of chemical bonding have been distinguished in some wide range of materials such as in Ca [49] and ZrNiAl alloy [51]. It has also been demonstrated that it is quite suitable to identify the site occupancy of H in these metals or alloys using ELF analysis [51].

The calculated ELF value reaches its maximum of 0.52 at the TIS in comparison with 0.42 and 0.48 at the respective OIS and DIS in the intrinsic Mo as shown in Fig. 3. As a matter of fact, when a H atom diffuses into a metal host, it will try to find a site with more localized electrons to achieve a more stable $1s^2$ valence electronic structure. The ELF value of more than 0.5 in an interstitial site implies that there exists relatively more paired electron feature, corresponding to nonbonding localized electrons in metallic environment [51]. Thus, we predict that the TIS (with the highest ELF value of 0.52) is preferred to be occupied by H, while the OIS and the DIS (with lower ELF value) are less possible for H to occupy. The ELF trend corresponds well to the relative stability of the TIS, the OIS, and the DIS (i.e., TIS > DIS > OIS) as obtained from the present calculation. This result again confirms the site occupancy rule of H in metals that H atom prefers to occupy the interstitial site where the ELF reaches the maxima [51].

3.2. Solubility of H in Mo

For the fusion application, H atoms are easily trapped directly into PFM such as Mo and W. The solubility plays a key role in determining the recombination rate coefficient [52], and should be directly associated with the H trapping and the bubble formation in Mo.

We can roughly estimate the dissolved concentration of H in Mo according to the Sieverts' law. The equilibrium H concentration in materials is defined as

$$C_H = \sqrt{(p/p_0)}\exp(\Delta S/k)\exp(-E_H^s/kT), \quad (3)$$

where p and p_0 are the background pressure and the reference pressure (here we choose standard pressure in order to make a comparison with the experiment), respectively. ΔS is called the solution entropy referred to the H_2 gas of the standard pressure, which is chosen as $-5.5\ k$ for H in Mo [53]. E_H^s is the solution energy of H in the TIS in Mo, and k and T are the Boltzmann constant and the absolute temperature, respectively. Using the calculated H solution energy of 0.62 eV and the experimental background pressure of $\sim 10^5$ Pa, we are able to determine the dissolved concentration of H in Mo.

Fig. 4 shows the dissolved concentration of H in Mo as a function of reciprocal temperature, in unit of the atomic fraction of H. We see that the H concentration has stronger temperature dependence, which increases with the temperature increasing, suggesting an endothermic reaction for the H dissolution in Mo. Oates and Mclellan measured the H dissolved concentration at the higher temperature case (1173–1773 K) in the earlier experiment [40], while Katsura recently gave the concentration results for relatively lower temperature case (723–1173 K) [41]. These results are also shown in Fig. 4. The present calculation results exhibit the similar trend to the experiments, but the absolute values are a bit different. The concrete values of the H dissolved concentration at typical temperatures (ranging from 600 K to 2000 K) are presented in Table 2. For example, the dissolved concentration is 2.6×10^{-8} at 600 K and 3.1×10^{-6} at 1000 K, respectively.

We can see that the actual concentration of H in the intrinsic Mo (e.g., only 2.6×10^{-8} at 600 K) is very low. This implies that the defect-free Mo cannot effectively trap H. Consequently, H will be difficult to accumulate and form bubbles, different from experimentally observed H blistering in Mo at 500 K [10,14]. The reason lies in that the defects such as vacancy and grain boundary in Mo have not taken into account. Under irradiation, a large amount of defects will be generated. In our previous studies, we have investigated the role of vacancy and grain boundary on the H trapping in W [6,28]. Both the vacancy and the grain boundary can act as the trapping centers which drive H to segregate toward these defects, leading to a large amount of H accumulation surrounding these defects. The experiment has shown that the vacancy should be responsible for the H trapping in Mo at the room temperature [14]. Relevant studies are in process.

3.3. Pairing of H in Mo

We now concentrate on the interaction of two H atoms in the intrinsic Mo. For two H atoms, different TIS's are respectively considered with different H–H distance, because the TIS is the most stable site for single H atom. We found that two H atoms tend to be paired up at two neighboring TIS, along the ⟨1 1 0⟩ directions

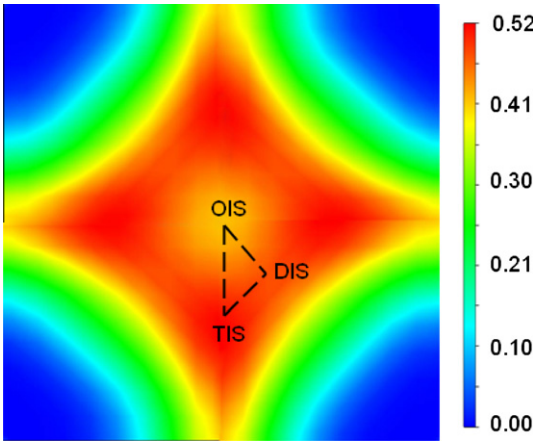

Fig. 3. The calculated electron localization function in the (0 0 1) plane of the intrinsic Mo.

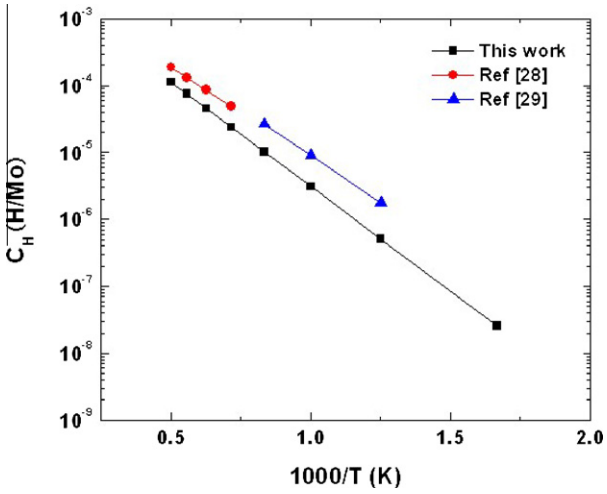

Fig. 4. The dissolved concentration of H in Mo as a function of reciprocal temperature in comparison with the previous experimental results.

Table 2
Dissolved concentration of H in Mo (C_H) at the different temperatures ranging from 600 K to 2000 K.

Temperature (K)	600	800	1000	1200	1400	1600	1800	2000
C_H (H/Mo)	2.6×10^{-8}	5.1×10^{-7}	3.1×10^{-6}	1.0×10^{-5}	2.4×10^{-5}	4.6×10^{-5}	7.5×10^{-5}	1.1×10^{-4}

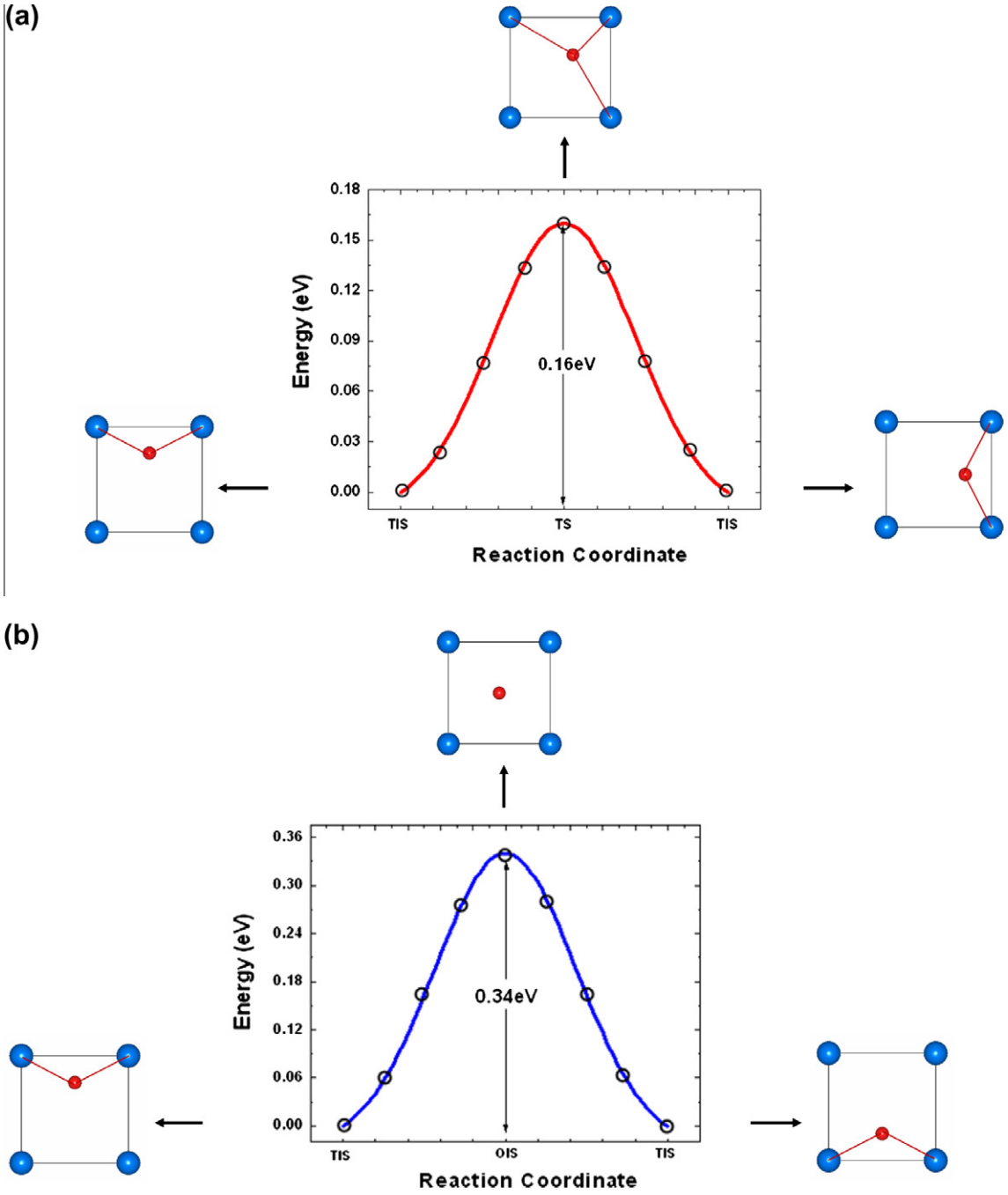

Fig. 5. Diffusion energy profile for the interstitial H atom in the intrinsic Mo. (a) T → T path and (b) T → O → T path.

with a small binding energy of 0.03 eV. The equilibrium distance of the H–H pair is ~0.221 nm. These are similar to the H pairing in W [5,6]. As a matter of fact, it is generally believed that the equilibrium distance between two H atoms in metals is difficult to be shorter than ~0.2 nm [54], otherwise a strong H–H repulsive interaction will occur. Moreover, such "~0.2 nm rule" appears to hold for the absolute majority of precisely described structure of metal and metal-alloys hydrides [55–57].

The distances of the H–H pair in Mo, however, are much longer than the H_2 bond length of ~0.075 nm and the interaction in such H–H pair is very weak with smaller binding energy of 0.03 eV, making two H atoms detach easily with increasing temperature. These suggest that two H atoms cannot bind together to directly form a H_2 molecule in the intrinsic Mo and thus form the H bubble. This notably differs from the behavior of helium (He) in metal, for which two He atoms will attract directly with each other and quite

easy to form He clusters with the large binding energy of 1.03 eV [58].

3.4. Diffusion of H in Mo

The diffusion properties are quite important for us to understand the behavior of H in Mo. On the one hand, the diffusion coefficient, as one of the most fundamental properties in materials, will affect the migration and the retention of H in Mo. On the other hand, the diffusion coefficient is also an important index to determine the diffusion velocity of H in Mo, which can help us to further understand the diffusion properties quantitatively. Therefore, we calculate the diffusion activation energy from the first-principles, based on which we are able to determine the diffusion coefficient of H in Mo.

We first calculate the activation energy for single H in the TIS that jumps to the nearest neighboring TIS via a mediate transition state configuration between two TIS's in the intrinsic Mo. We use a drag method similar to the previous studies [5,6,59]. The preferred diffusion path for H is via one TIS to the first nearest neighbor (1NN) TIS directly (T → T path), as shown in Fig. 5a, with a much lower activation energy of 0.16 eV. This value basically agrees with the previously reported experimental activation energy of 0.17 eV [41] and 0.23 eV [60]. The difference is attributed to the introduction of vacancy and other defects in the experiment which can act as an effective trap for H and thus to some extent reduce its mobility [28].

In addition, we also investigate another possible diffusion path in which H moves from one TIS to the 2NN TIS via a middle OIS (T → O → T path). The activation energy for this path is calculated to be 0.34 eV (Fig. 5b), which is almost the energy difference between OIS and TIS. We note that such T → O → T path might contribute to the mobility of H at the higher temperature due to the higher activation energy in comparison with the T → T path.

Next, we investigate the diffusion coefficient of H in Mo. The diffusion coefficient of H atom can be obtained by the Arrhenius diffusion equation $D = D_0 \exp(-E_a/kT)$, where D_0 and E_a are the pre-exponential factor and the activation energy of H atom, respectively. For a metal with a cubic structure, D_0 can be expressed as $D_0 = \frac{1}{6}a^2\nu$, where a and ν are the lattice constant and the vibration frequency, respectively.

The vibration frequency ν of the interstitial H can be determined according to Zener and Wert's theory [61]. In this theory, ν can be approximately expressed by $\nu = \sqrt{2E_a/ma^2}$, where m is the mass of the H atom. Using the mass of H atom of 1.66×10^{-27} kg and the Mo lattice constant of 0.316 nm together with the calculated H activation energy of 0.16 eV, we can thus obtain the vibration frequency $\nu = 1.76 \times 10^{13}$ Hz. Substituting this value into the diffusion equation, the pre-exponential factor D_0 is obtained to be 2.93×10^{-7} m^2/s.

After establishing the pre-exponential factors, the diffusion coefficient of H in Mo can be calculated according to the Arrhenius equation as mentioned above. Fig. 6 shows the diffusion coefficient of H as a function of reciprocal temperature. Our calculations predict that the diffusion coefficient of H can be expressed by $D = 2.93 \times 10^{-7} \exp(-0.16eV/kT)$ m^2/s. The corresponding values at the different temperatures ranging from 600 K to 2000 K are listed in Table 3. At 600 K and 1000 K, the diffusion coefficients are 1.3×10^{-7} m^2/s and 4.6×10^{-7} m^2/s, respectively.

H and its isotopes D and T will exhibit different diffusion behaviors due to their different masses. The corresponding relation between D_0 and m is $D_0 = \frac{1}{6}a^2\sqrt{2E_a/ma^2}$ as indicated above. Based on the pre-exponential factors of D and T that are calculated to be 2.07×10^{-7} m^2/s and 1.69×10^{-7} m^2/s, we can obtain the diffusion coefficients of D and T. Table 3 shows the diffusion coefficients of D and T at the temperature range of 600 K to 2000 K. One sees that the T diffusion coefficient is the lowest among H, D, and T. Clearly, different masses of H isotopes result in different diffusion coefficients and thus different retention.

For H in a metal, it is well known that there exists an obvious character of fugacity even at the room temperature, i.e., H can easily migrate in the bulk [4]. The present results for both the lower H diffusion energy barrier and the weaker interaction of double H atoms suggest a high mobility of H in Mo.

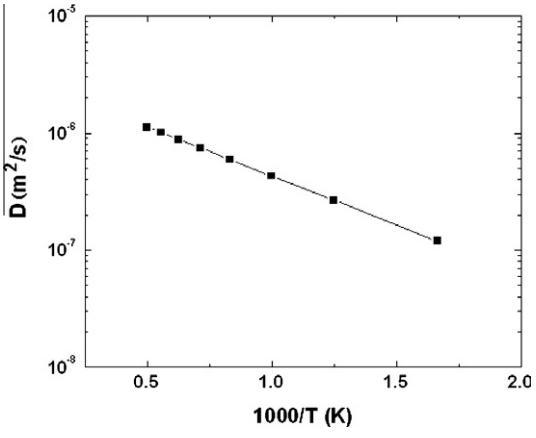

Fig. 6. Diffusion coefficient of H in Mo via the T–T path as a function of reciprocal temperature.

4. Summary

We have investigated dissolution and diffusion properties of hydrogen (H) in molybdenum (Mo), one of the important candidates for the plasma facing material (PFM) in a nuclear fusion Tokamak, using a first-principles method. We show that single H atom is energetically favorable sitting at the tetrahedral interstitial site (TIS) instead of the octahedral interstitial site (OIS) and the diagonal interstitial site (DIS). The solution energy of single H at the TIS is calculated as 0.62 eV in comparison with 0.74 eV and 0.94 eV at the OIS and the DIS, respectively, which indicates the endothermic reactions for all these cases. The electron localization function further confirms the energetic results and can be used to correctly predict the site occupancy of H. The calculated Bader charge is −0.79 e for H at the TIS, suggesting formation of the ionic and slight covalent mixing bonding between H and surrounding Mo. Using the Sieverts' law, we estimate the dissolved concentration of H in Mo, which are 2.6×10^{-8} and 3.1×10^{-6} at the typical temperatures of 600 K and 1000 K, respectively. The dissolved con-

Table 3
Diffusion coefficients of H, D, and T in Mo in the unit of m^2/s at the different temperatures ranging from 600 K to 2000 K.

Temperature (K)	600	800	1000	1200	1400	1600	1800	2000
H	1.3×10^{-7}	2.9×10^{-7}	4.6×10^{-7}	6.2×10^{-7}	7.8×10^{-7}	9.2×10^{-7}	1.0×10^{-6}	1.2×10^{-6}
D	9.2×10^{-8}	2.1×10^{-7}	3.3×10^{-7}	4.4×10^{-7}	5.5×10^{-7}	6.5×10^{-7}	7.1×10^{-7}	8.5×10^{-7}
T	7.5×10^{-8}	1.7×10^{-7}	2.7×10^{-7}	3.6×10^{-7}	4.5×10^{-7}	5.3×10^{-7}	5.8×10^{-7}	6.9×10^{-7}

centration results are basically consistent with the experiments. Double H atoms tend to be paired up at the two neighboring TIS along the ⟨1 1 0⟩ direction with a distance of ~0.221 nm and a binding energy of 0.03 eV. This suggests a weak attractive interaction between H atoms, with the implication that self-trapping of H and thus formation of the H_2 molecules are almost impossible in an intrinsic Mo environment. We demonstrate that the diffusion barrier of H that jumps between the neighboring TIS's is ~0.16 eV, in good accordance with experimental results. The diffusion coefficients of H, D, and T are different due to the different masses, which are calculated to be 1.3×10^{-7} m^2/s, 9.2×10^{-8} m^2/s, and 7.5×10^{-8} m^2/s at a typical temperature of 600 K.

Acknowledgement

This research is supported by National Magnetic Controlled Fusion Program with Grant No. 2009GB106003.

References

[1] B. Magyari-Kope, V. Ozolins, C. Wolverton, Phys. Rev. B 73 (2006) 220101.
[2] S. Li, P. Jena, R. Ahuja, Phys. Rev. B 73 (2006) 214107.
[3] A.R. Troiano, Trans. Am. Soc. Method 52 (1960) 54.
[4] J.B. Condon, T.J. Schober, J. Nucl. Mater. 207 (1993) 1.
[5] Y.-L. Liu, Y. Zhang, G.-N. Luo, et al., J. Nucl. Mater. 390–391 (2009) 1032.
[6] H.-B. Zhou, Y.-L. Liu, Y. Zhang, et al., Nucl. Fusion 50 (2010) 025016.
[7] The fusion energy is being developed internationally via the ITER (International Thermonuclear Experimental Reactor) Project.
[8] R. Causey, K. Wilson, T. Venhaus, et al., J. Nucl. Mater. 266–269 (1999) 467.
[9] G.-N. Luo, W.M. Shu, M. Nishi, J. Nucl. Mater. 347 (2005) 111.
[10] J.P. Sharpe, R.D. Kolasinski, M. Shimada, et al., J. Nucl. Mater. 390–391 (2009) 709.
[11] R.A. Causey, C.L. Kunz, D.F. Cowgill, J. Nucl. Mater. 337–339 (2005) 600.
[12] C.H. Wu, U. Mszanowski, J. Nucl. Mater. 218 (1995) 293.
[13] W.R. Wampler, B. LaBombard, J. Nucl. Mater. 266–269 (1999) 217.
[14] S. Nagata, K. Takahiro, J. Nucl. Mater. 283–287 (2000) 1038–1042.
[15] S. Nagata, K. Takahiro, J. Nucl. Mater. 266–269 (1999) 1151.
[16] G.M. Wright, D.G. Whyte, B. Lipschultz, J. Nucl. Mater. 390–391 (2009) 544–549.
[17] T. Tanabe, H. Hachino, M. Takeo, J. Nucl. Mater. 176–177 (1990) 666.
[18] T. Hoshihira, T. Otsuka, T. Tanabe, J. Nucl. Mater. 386–388 (2009) 776.
[19] T. Hoshihira, T. Otsuka, T. Tanabe, J. Nucl. Mater. 390–391 (2009) 1029.
[20] C. Wert, C. Zener, Phys. Rev. 76 (1949) 1169.
[21] P. Nordlander, J.K. Norskov, F. Besenbacher, et al., Phys. Rev. B 40 (1989) 1990.
[22] J.K. Norskov, F. Besenbacher, J. Less-Common Met. 130 (1987) 475.
[23] P. Nordlander, J.K. Norskov, F. Besenbacher, J. Phys. F 16 (1986) 1161.
[24] S.M. Myers, P. Nordlander, F. Besenbacher, et al., Phys. Rev. B 33 (1986) 854.
[25] F. Besenbacher, S.M. Myers, P. Nordlander, et al., J. Appl. Phys. 61 (1987) 1788.
[26] J. Cizek, I. Prochazka, F. BeŁvał, et al., Phys. Rev. B 69 (2004) 224106.
[27] S.T. Picraux, F.L. Vook, Phys. Rev. Lett. 33 (1974) 1216.
[28] Y.-L. Liu, Y. Zhang, H.-B. Zhou, et al., Phys. Rev. B 79 (2009) 172103.
[29] Y. Fukai, N. Okuma, Phys. Rev. Lett. 73 (1994) 1640.
[30] Y. Fukai, Phys. Scripta T103 (2003) 11.
[31] G. Lu, E. Kaxiras, Phys. Rev. Lett. 94 (2005) 155501.
[32] S. Li, P. Jena, R. Ahuja, Phys. Rev. B 72 (2005) 174116.
[33] Y. Fukai, J. Alloys Compd. 356–357 (2003) 263.
[34] G. Kresse, J. Hafner, Phys. Rev. B 47 (1993) 558.
[35] G. Kresse, J. Furthmüller, Phys. Rev. B 54 (1996) 11169.
[36] J.P. Perdew, Y. Wang, Phys. Rev. B 45 (1992) 13244.
[37] P.E. Blochl, Phys. Rev. B 50 (1994) 17953.
[38] H.J. Monkhorst, J.D. Pack, Phys. Rev. B 13 (1976) 5188.
[39] C. Kittel, Introduction to Solid State Physics, seventh ed, Wiley, New York, 1996.
[40] W.A. Oates, R.B. Mclellan, Scr. Metall. 6 (1972) 349.
[41] H. Katsura, T. Iwai, H. Ohno, J. Nucl. Mater. 115 (1983) 206.
[42] Y.-L. Liu, H.-B. Zhou, Shuo Jin, et al., Phys. Rev. B submitted for publication.
[43] M.J. Puska, R.M. Nieminen, M. Manninen, Phys. Rev. B 24 (1981) 3037.
[44] J.K. Norskov, Phys. Rev. B 26 (1982) 2875.
[45] R.W.F. Bader, Atoms in Molecules: A Quantum Theory, Oxford University Press, Oxford, 1990.
[46] G. Henkelman, A. Arnaldsson, H. Jónsson, Comput. Mater. Sci. 36 (2006) 354.
[47] E. Sanville, S.D. Kenny, R. Smith, et al., J. Comput. Chem. 28 (2007) 899.
[48] J.K. Norskov, Phys. Rev. B 20 (1979) 446.
[49] A. Savin, R. Nesper, S. Wengert, et al., Angew. Chem. Int. Ed. Engl. 36 (1999) 1808.
[50] M. Kohout, A. Savin, J. Comput. Chem. 18 (1997) 1431.
[51] P. Vajeeston, P. Ravindran, R. Vidya, et al., Europhys. Lett. 72 (2005) 569.
[52] R. Causey, J. Nucl. Mater. 300 (2002) 91.
[53] Y. Fukai, The Metal-Hydrogen System, Springer, Berlin, 1993.
[54] A.C. Switendick, Z. Phys. Chem. 117 (1979) 89.
[55] B.K. Rao, P. Jena, Phys. Rev. B 31 (1985) 6726.
[56] H. Smithson, C.A. Marianetti, D. Morgan, et al., Phys. Rev. B 66 (2002) 144107.
[57] H. Wu, W. Zhou, T.J. Udovic, et al., Phys. Rev. B 75 (2007) 064105.
[58] C.S. Becquart, C. Domain, Phys. Rev. Lett. 97 (2006) 196402.
[59] C.C. Fu, F. Willaime, P. Ordejon, Phys. Rev. Lett. 92 (2004) 175503.
[60] T. Tanabe, T. Yamanishi, S. Imoto, J. Nucl. Mater. 191–194 (1992) 439.
[61] R. Frauenfelder, J. Vac. Sci. Technol. 6 (1969) 388.